

Understanding Imaging and Metrology with the Helium Ion Microscope

Michael T. Postek, András E. Vladár and Bin Ming^[1, 2]

*Precision Engineering Division
Manufacturing Engineering Laboratory
National Institute of Standards and Technology,
100 Bureau Drive MS 8210
Gaithersburg, MD 20899*

Abstract. One barrier to innovation confronting all phases of nanotechnology is the lack of accurate metrology for the characterization of nanomaterials. Ultra-high resolution microscopy is a key technology needed to achieve this goal. But, current microscope technology is being pushed to its limits. The scanning and transmission electron microscopes have incrementally improved in performance and other scanned probe technologies such as atomic force microscopy, scanning tunneling microscopy and focused ion beam microscopes have all been applied to nanotechnology with various levels of success. A relatively new tool for nanotechnology is the scanning helium ion microscope (HIM). The HIM is a new complementary imaging and metrology technology for nanotechnology which may be able to push the current resolution barrier lower. But, successful imaging and metrology with this instrument entails new ion beam/specimen interaction physics which must be fully understood. As a new methodology, HIM is beginning to show promise and the abundance of potentially advantageous applications for nanotechnology have yet to be fully exploited. This presentation will discuss some of the progress made at NIST in understanding the science behind this new technique.

Keywords: Helium ion, microscope, HIM, scanning electron microscope, SEM, nanomanufacturing, nanometrology

PACS: 68.37.Hk, 07.78.+s, 41.85.-p

INTRODUCTION

The lack of accurate metrology for the characterization of nanomaterials is one barrier to innovation confronting all phases of nanotechnology. Ultra-high resolution microscopy is a key technology needed to achieve this goal. But, current microscope technology is being pushed to its limits. [3, 4, 5] The scanning and transmission electron microscopes have incrementally improved in performance and other scanned probe technologies such as atomic force microscopy, scanning tunneling microscopy and focused ion beam microscopy have all been applied to nanotechnology with various levels of success. Evolution of the technology has been steady and highly responsive to the needs of the research community.

A new tool for nanotechnology is the scanning helium ion microscope (HIM). As reported in earlier papers [6, 7, 8, 9], the HIM is a new approach to imaging and metrology for nanotechnology which may

be able to push the current resolution barrier lower. This instrument also promises the potential for new imaging modes, as well as, charge free imaging without the need for conductive coating. But, successful imaging and metrology with this instrument entails new ion beam/specimen interaction physics which must be fully understood. As a new methodology, HIM is beginning to show promise and the abundance of potentially advantageous applications for nanotechnology have yet to be fully exploited. NIST was fortunate to receive the first commercial HIM [7] and this paper will discuss some of the progress made at NIST in improving its performance and to understand the science and capabilities of this new instrumentation. In addition, it is the NIST goal to understand potential differences between HIM and contemporary scanning electron microscope (SEM) instruments. Clearly, this is a difficult task since the SEM and the HIM appear similar in that both are scanned particle beam instruments but are quite different in their operational parameters.

MATERIALS AND METHODS

The scanning helium ion microscopes used in this work were either a Zeiss Orion Plus installed in the NIST Advanced Measurement Laboratory or an engineering instrument installed at the Zeiss facility in Peabody, MA.

QUEST FOR ULTRA-HIGH RESOLUTION

Ultra-high instrument resolution is the “holy grail” of scanning electron and ion microscopy. The goal is to be able to image and measure the smallest details on the samples being viewed. Table 1 shows the manufacturer specified resolution values of four contemporary scanning electron and ion microscopes installed within the Precision Engineering Division (PED) of NIST. The methods used in obtaining these specification numbers are diverse and none of them

perform better than at low accelerating voltage. There are a number of reasons for this characteristic difference [12] but, is not the subject of this work. In the SEM, low landing energies are commonly employed when surface information is desired. But, the compromise is lower attainable resolution. For example, an SEM operating at 15 kV accelerating voltage will potentially have better than 1 nm performance, but that same SEM operating at 1.0 kV will perform at about 1.5 nm (or more). Newer aberration corrected SEM instruments have improved this situation and higher resolution low landing energy images now can be obtained in the subnanometer region. On the other hand, surface detail can be resolved with the HIM (discussed below) but, the current HIM instruments typically function only at high landing energies. So it must be understood that direct comparisons between the performance of the HIM and SEM are rather difficult to do today even under high landing energy conditions.

TABLE 1. Resolution of PED Scanning Electron and Ion Microscopes*

| Instrument | Manufacturer Specification | Best Measured Resolution | Median of Measured Resolution |
|-------------------|-----------------------------------|---------------------------------|--------------------------------------|
| 1 | 0.9 nm | 0.65 nm | 0.78 nm |
| 2 | 0.4 nm | 0.38 nm | 0.42 nm |
| 3 | 0.8 nm | 0.7 nm | 1.2 nm |
| 4 | 1.0 nm | 0.8 nm | 0.9 nm |

*Manufacturer’s names intentionally omitted

are truly traceable to internationally accepted standards – today [10]. But, they can be used for comparative purposes; all of these data were taken with the optimum high landing energy and instrument operational parameters. Standardization for instrument performance is one of the goals of the NIST Manufacturing Engineering Laboratory’s Nanomanufacturing and Next-Generation Metrology Programs for which understanding the overall behavior of the individual instruments is highly critical. The methods used to derive the NIST instrument’s data in the table are described elsewhere [11]. The four instruments measured all reside in environmentally stable laboratories within the NIST Advanced Measurement Laboratory. All of the manufacturers have generously collaborated with NIST to maintain these instruments at the highest possible levels of performance.

Ultimate instrument resolution relates directly to the landing energy. It is well known that at high accelerating voltages, particle beam instruments

Clearly, the ability to resolve fine detail with all particle beam microscopes has drastically improved over the past 20 years. The resolution achievable with the newest SEMs has been published by the manufacturer to be at or below 0.4 nm [13] and for the scanning helium ion microscope, 0.21 nm has been reported [14]. To put this into perspective, the {111} crystal plane in silicon (Si) has a 0.32 nm lattice spacing, so only a very few atoms are located within a cubic nanometer of the Si crystal. Even the best of the current instruments must perform at the highest level possible to resolve routinely the finest structures of nanomaterials.

Attaining high resolution depends directly on a number of factors such as: a) the physics of the particle beam; b) the electromagnetic focusing ability of the electron or ion-optical column; c) the size and shape of the best focused beam, d) the conical angle of the beam; and e) overall signal-to-noise ratio. Resolution is also directly related to the sample being analyzed since the size and shape of the information

volume is the region of the excited volume where the collected (generally) secondary electron (SE) signal originates. Therefore, the apparent sharpness of the image obtained will be a function of the material being analyzed and not necessarily the instrument performance. Moreover, the amount of noise present in the system plays an important role as well, because it limits the amount of information recoverable from the image generated by the microscope. In most cases, much of this is transparent to the user and, in almost all practical instances; the focusing ability of the optical column is not the limiting factor because other contributory factors (e.g., operator ability, environmental effects, sample contamination, electromagnetic fields, sample stage and beam drift, and vibration) also at work to reduce the achievable instrument resolution.

The Primary Electron and Ion Beams and Excited Volumes

The scanning electron microscope and the helium ion microscope share a number of fundamental characteristics. Figure 1 shows an idealized representation of the electron or ion beam. The primary electron or ion beam is composed of a three-dimensional distribution of electrons or ions along and across the beam. The beam is generally thought to have a somewhat double-conical shape, with the important half-angle parameter that defines the depth-of-field and the disk of least confusion where the best focus (i.e. the smallest spot size) can be achieved.

Depth-of-Field

Figure 1 shows a diagrammatic representation of the beam relative to a nano-structure. In this diagram, a 3 nm difference in the beam diameter at the top and at the bottom of the 100 nm structure is shown. A more parallel beam results in a smaller difference hence, better depth-of-field. Under normal operating conditions, the HIM - where the source of ions begins at single atom [6, 7, 8, 9] - can result in a narrower convergence angle than the SEM (depending upon the instrument operating conditions). Therefore, the overall depth-of-field can be larger than the SEM even at higher magnifications [8, 15]. The difference in the depth-of-field is illustrated in the micrographs of Figure 2. The top pair depicts the comparison between SEM (left) and HIM (right) and the bottom pair of Figure 2 is a digital enlargement showing that the end of the 1 mm long channel is still in focus in the HIM image, but the SEM image is not sharp and is out of focus. In certain cases, using the most optimum conditions and instrument settings, the depth-of-field of the HIM can be 5 times greater than the SEM.

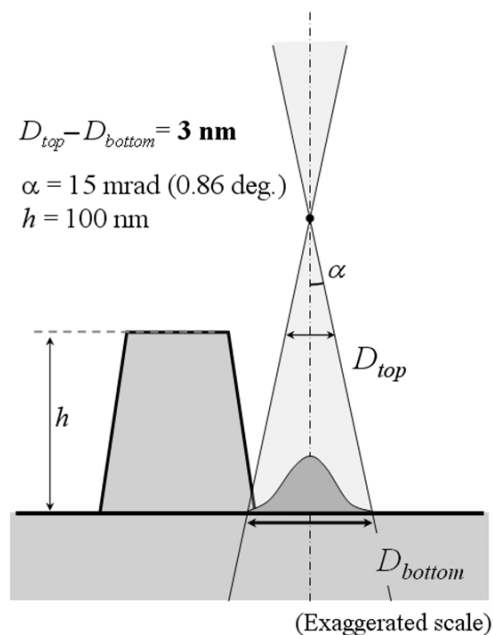


FIGURE 1. Idealized diagram of an electron or ion beam with a double-conical shape and Gaussian electron or ion intensity distribution across the beam. Note that the scales depicted have been exaggerated. (Courtesy of M. Tanaka of Hitachi High Technologies).

Signal

The signal composing the image from the SEM or the HIM is a complex product of: a) the interaction of the electron or ion probe with the sample, b) the composition of the sample, c) sample chamber geometry and chamber material, d) and the electromagnetic field present around the sample (either from the instrument itself or from sample biasing and/or charging). The three-dimensional electron or ion beam and the sample define this 3-D information volume. This is the 3-D region from which the detected signals originate. Therefore, although imaging in the SEM or HIM appears straightforward, it is in reality a rather complex affair (as discussed further below). Additionally, for accurate dimensional measurements at the nanometer scale, sophisticated modeling methods that account for all the physical processes must be used to measure accurately the shape and size of the sample structures of interest [15, 16, 17, 18]. Ramachandra et al., [18] have developed the IONiSE Monte Carlo model to predict the topographic yield variation of helium generated SE as a function of sample composition. With this model, the important details of helium ion SE imaging can be compared with comparable electron-generated SE imaging. Such work is an important and primary step in the understanding of the imaging and metrology of the HIM.

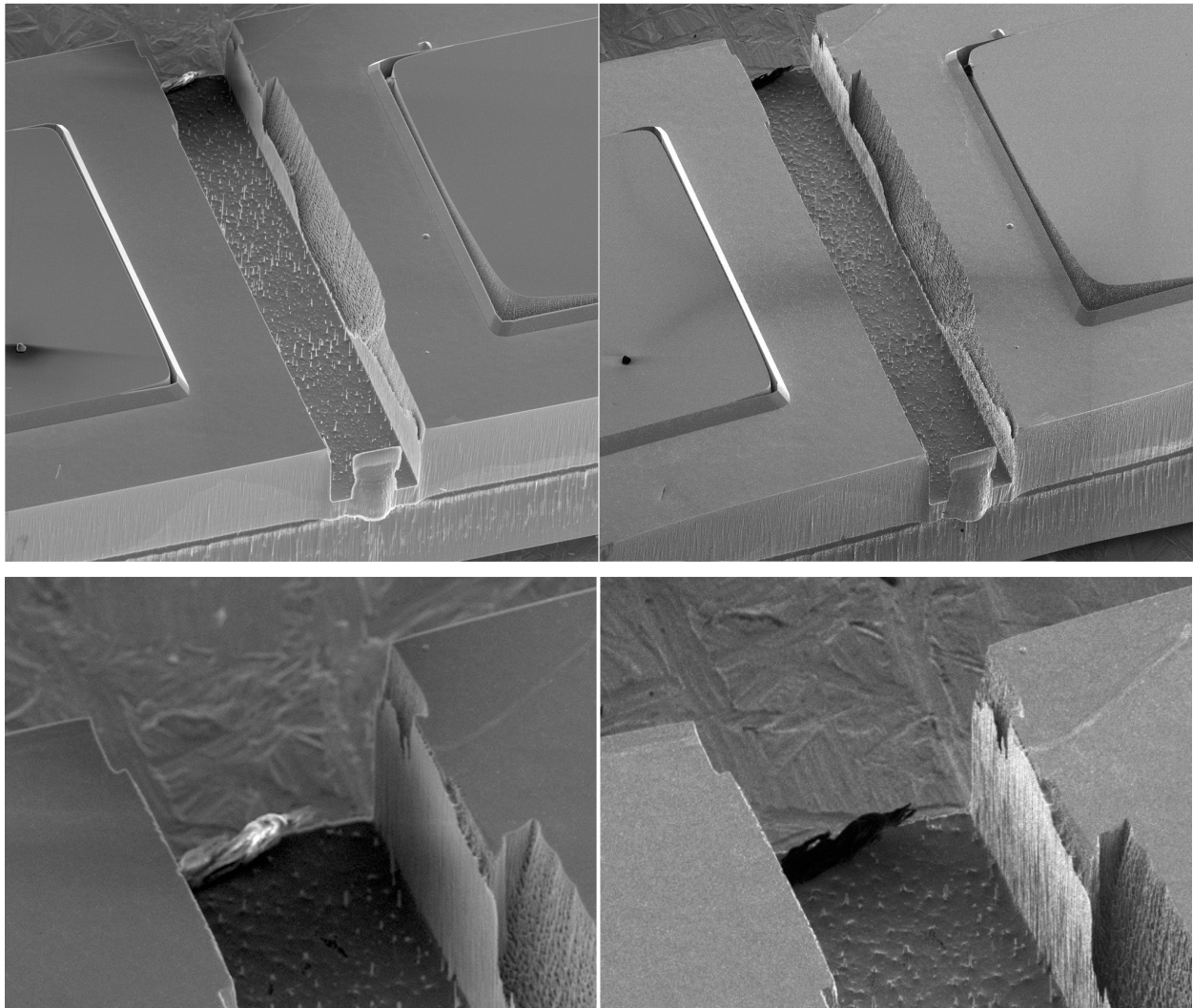


FIGURE 2. Top: Depth-of-field comparison between the scanning electron microscope (left) and the helium ion microscope (right) on an etched Si cantilever sample. The field-of-view is = 1 mm. Bottom: Depth of field comparison of the SEM (left) and the HIM (right) image portions after *digital* magnification increase. Note the lack of sharpness of the SEM image. The field-of-view is = 312 μm

Excited Volume

The current understanding is that the volume excited by the electron beam in the SEM and the volume excited by the HIM are quite different [6]. Figure 3 illustrates a comparison of the electron beam interaction data from the Monte Carlo program CASINO 2.42 (left) and ion beam interaction data modeled by SRIM 2008.04 (right). In both instances, 30 keV particles are interacting with an infinitely thick silicon (Si) sample. Note the fundamental difference in the interaction volumes. This volume is where the important beam-specimen interactions take place and it has been documented experimentally for the SEM [19, 20] but has not been done, as of yet, for the HIM.

Within the excited volume, the SE escape depth is the region from which the secondary electrons have enough energy to leave the sample surface to be potentially collected. The escape depth can be a few nm to up to more than 10 nm, depending on the sample material. For metals it is thinner, for insulators it is generally larger. The shape and size, the depth reached by electrons and ions and the secondary electron generation efficiency all strongly depend on the landing energy of the electrons or ions and the sample material irradiated. The landing energy of electrons in an SEM is variable; however, adjustable ion acceleration in the HIM is a capability still being implemented.

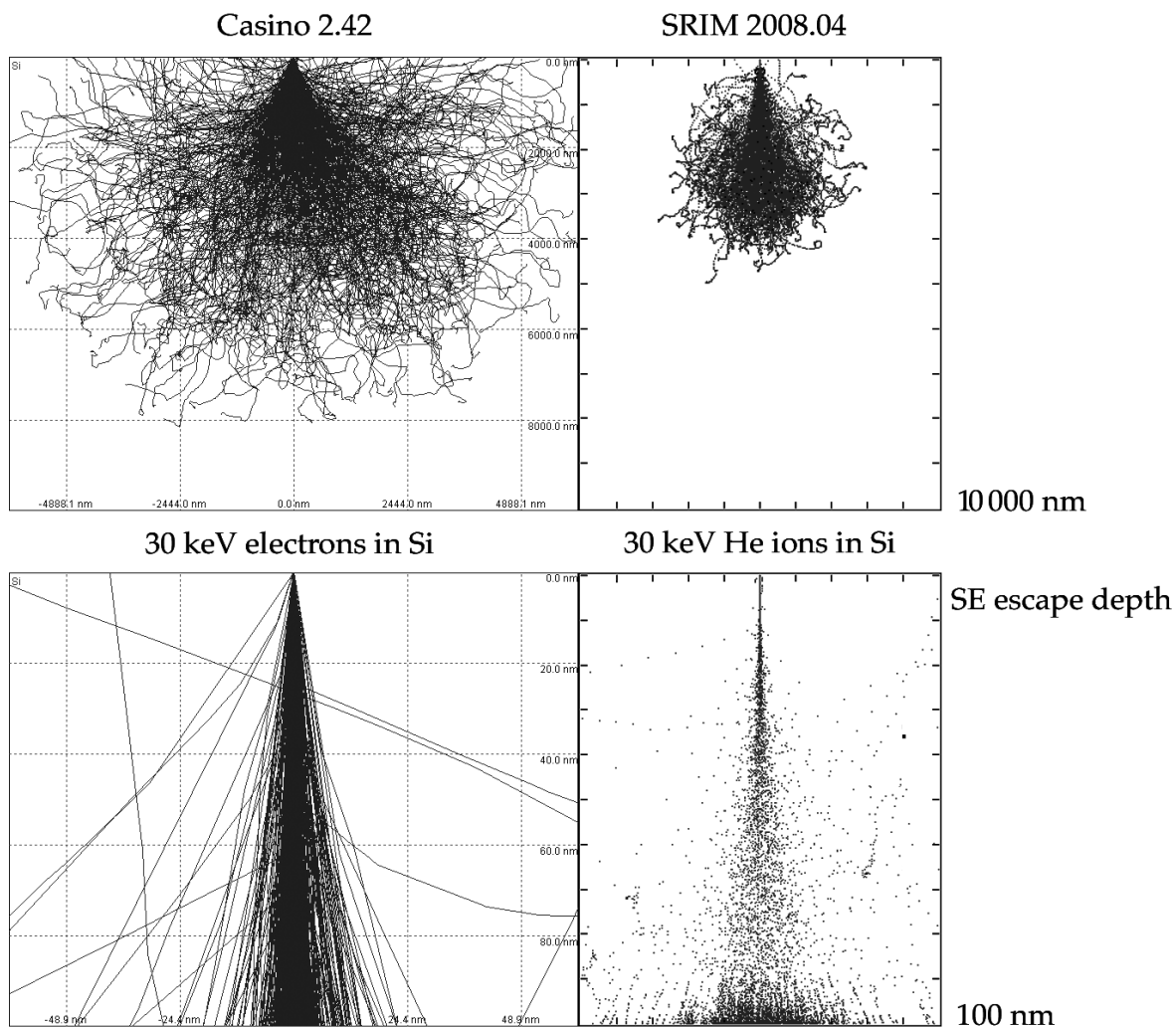


FIGURE 3. Comparison of the electron beam interaction data from the Monte Carlo program CASINO 2.42 (left) and ion beam interaction data modeled by SRIM 2008.04 (right). In both instances, 30 keV particles are interacting with an infinitely thick silicon (Si) sample. Note the fundamental difference in the interaction volumes. The SE escape depth is the narrow region from where the secondary electrons have enough energy to leave the sample surface.

The size and shape of the excited and information volumes along with the secondary electron generation efficiency and location are important for another reason. The amount of surface-related information collected is directly dependent on these factors. Those secondary electrons carrying information about the finest details of the sample are generated by the primary electrons or ions at the point where the beam hits the sample. These are the so-called type SE1 electrons. The secondary electrons that were created by energetic electrons or ions backscattered within the sample are designated as SE2. Because of the location

of their generation, the SE2 do not carry information about finest sample details; in fact, it is clearly shown in Figure 3 (left) that current modeling shows that many more electrons emerge remotely from the initial point of primary electron interaction than shown in the modeled data from the ion beam. The size of this area depends on the primary excitation and the material composing the sample under examination and can extend more than a micrometer in diameter [21]. Electrons are also generated by the backscattered electrons or ions that leave the sample and hit some other material within the sample chamber. These secondary electrons are called SE3. Again, these do

not carry information about finest sample details. The well-focused beam always generates SE1, but the relative amounts of SE1 and SE2 and SE3 electrons have a profound effect on the appearance and the amount of fine details resolved in the secondary electron image. Peters [22] measured the individual contributions of the components of the SE signal, in the SEM, from gold crystals and found that, depending upon the sample viewed, the total SE image the contribution of the SE2 is approximately 30% and the contribution to the image of the SE3 electrons is approximately 60% as compared with approximately 10% of the image contributed by the SE1 derived signal. This ratio of SE2/SE1 generated by electrons [18, 23, 24, 25] significantly reduces the contrast and resolvability of small features. Clearly, this depends on landing energy and SE and backscattered electron or ion yields.

In the HIM, secondary electrons forming the image are produced at (or very near, within the escape depth of the SEs) the point of initial interaction with the sample and thus, are equivalent to SE1 electrons of the SEM. The initial SEs produce images with strong and familiar topographic contrast, and generally appear very similar to the secondary electron images obtained from an SEM, upon first inspection. IONiSE modeling [17, 18] predicts that the helium-ion-generated SE2/SE1 ratio should be lower than that for electron irradiation especially at the higher landing energies. Hence, the contrast and the surface details are enhanced. Contrary to the SEM interactions, the ion beam passes much more deeply into the sample matrix (Figure 3) and very few SE2 or SE3 type electrons dominant in the SEM imaging are generated. The flood of SE2 and SE3 electrons resulting from the backscatter of electrons in the SEM can essentially “wash-out” the surface detail potentially resolved by the electron beam. This does not occur to the same extent in the HIM, resulting in the enhanced surface detail as shown in Figure 4. Thus, in a material infinitely thicker than the secondary electron escape depth, clear surface detail may be resolved. This can be exemplified by the ability to image very thin layers of ion evaporated gold on a silicon surface as shown in Figure 5. In this figure, sufficient ion beam current was applied to a small gold particle to evaporate it in the direction of the tilt plane. The gold was then deposited as a thin layer which can be readily observed as a crescent shape extending down the tilt plane. In the SEM, under similar conditions the thin film would likely not be observed because of the flux of SE2 and SE3 electrons.

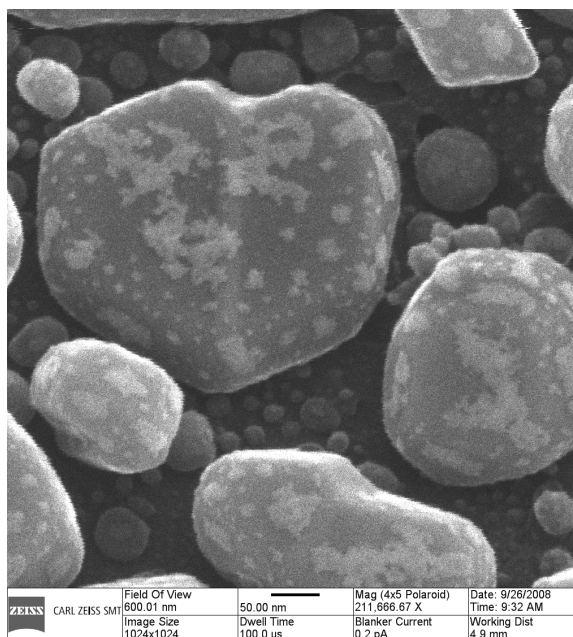


FIGURE 4. HIM micrograph of a gold-on-carbon resolution sample showing fine detail on the surface of the gold islands which is not typically observed in the SEM images. The field-of-view = 600 nm.

Sub-surface contributions to the HIM image are also possible. In very thin materials, low in atomic number or those that are flocculent, significant contributions to the image can be made from underlying structures (Figure 6). The SEM or HIM beam enters the first layer of the sample and generates signal then passes through (potentially generating signal, as well) striking another fiber or portion of the sample also generating signal. The sum of both is collected by the secondary electron detector resulting in an image such as the one shown in Figure 6. In this figure, one interpretation of this image is that the ion beam penetrated through the initial thin fiber providing signal from both the upper and lower fibers of the sample. Other possible mechanisms for generating sub-surface signal may be from electron channeling effects. Further research into these mechanisms and the underlying physics needs to be done in order to understand fully these observations. For now, adjusting instrument operating conditions helps to minimize these contributions.

Helium Ion Beam Milling and Sample Damage

Depending upon the beam current, the flux of particles within the excited volume of either the SEM or the HIM can be substantial and can lead to significant sample degradation [26]. Moreover, much of the energy of the primary electrons or ions stays within the sample, which can cause adverse effects

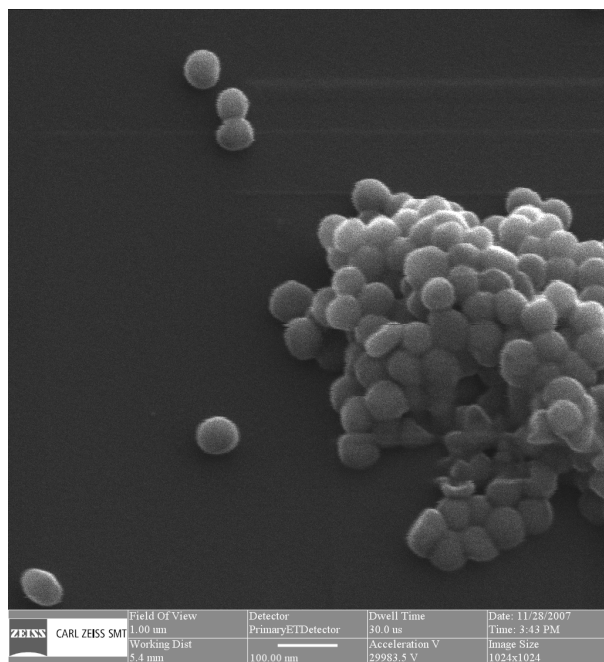
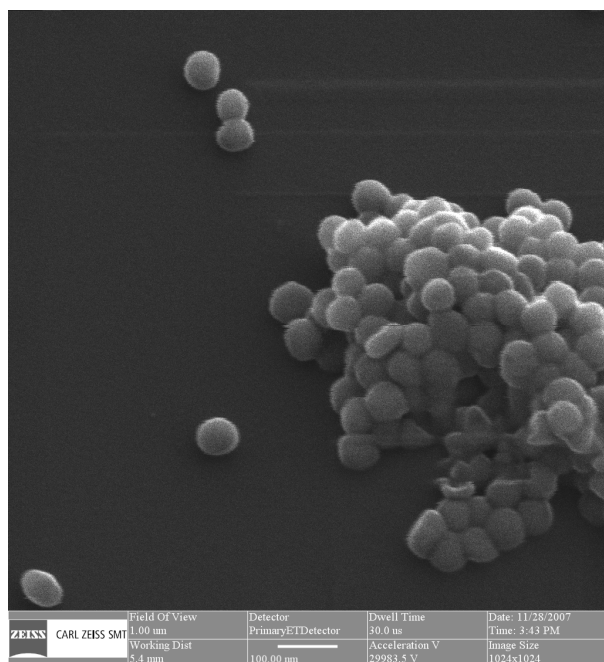


FIGURE 5. HIM image of intact gold particles (upper) and the same particles evaporated (lower) showing the deposition of the gold in the direction of the tilt plane (top of the frame). The evaporated gold from the particles is seen as a very thin deposit of a brighter grey indicating different atomic number. The field-of-view is 1µm.

such as sample melting, swelling or other dimensional changes. This is not to say that the electron and ion are equivalent in their effects. An electron stopping in a sample does not occupy a significant volume;

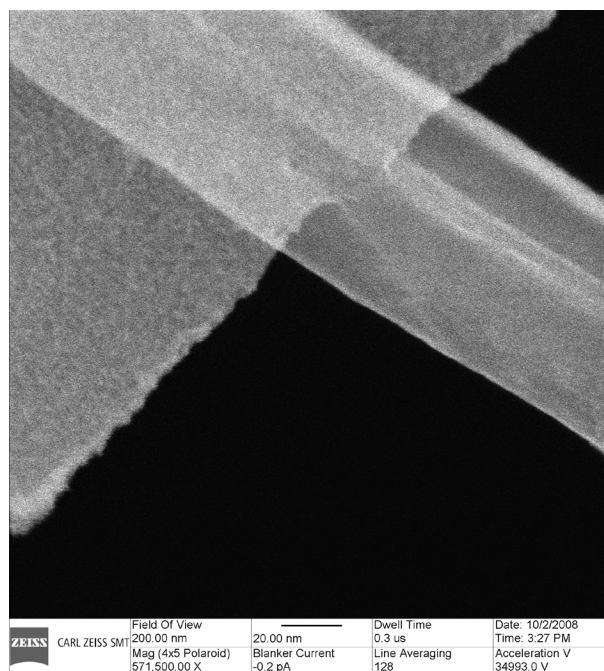


FIGURE 6. HIM image of asbestos fibers showing the “ghosting” effect generated by beam penetration through the initial fiber and into to the underlying fibers. The initial particle is sufficiently thin to permit signal contribution from underlying structures. The secondary electrons from both structures are essentially summed into the image. The field-of-view = 200 nm.

however, the larger helium ions remaining in the sample could result in a swelling of the structures. However, this is highly sample dependent; multiple imaging of robust structures shows no swelling or detrimental modifications to the structure under observation. However, this effect needs to be studied in greater detail. Unwanted sample modification is an issue which is a function of the material being viewed and the operating conditions of the instrument (beam current, accelerating voltage, etc.). It is up to the operator to find the optimal imaging and measurement conditions to obtain the best and repeatable results. For the scanning electron microscope many years of experience has provided some of the answers to sample damage for the SEM, but the HIM is still a new development and much has yet to be learned.

Gallium ion microscopes are well known for their ability to perform ion beam milling of samples for a vast array of purposes including transmission electron microscope (TEM) sample preparation. The helium ion microscope can also be used for focused ion beam mediated material removal by adjusting the instrument parameters and increasing the beam current and dwell time. Because of the inherently small source size, the HIM has demonstrated very fine material removal.

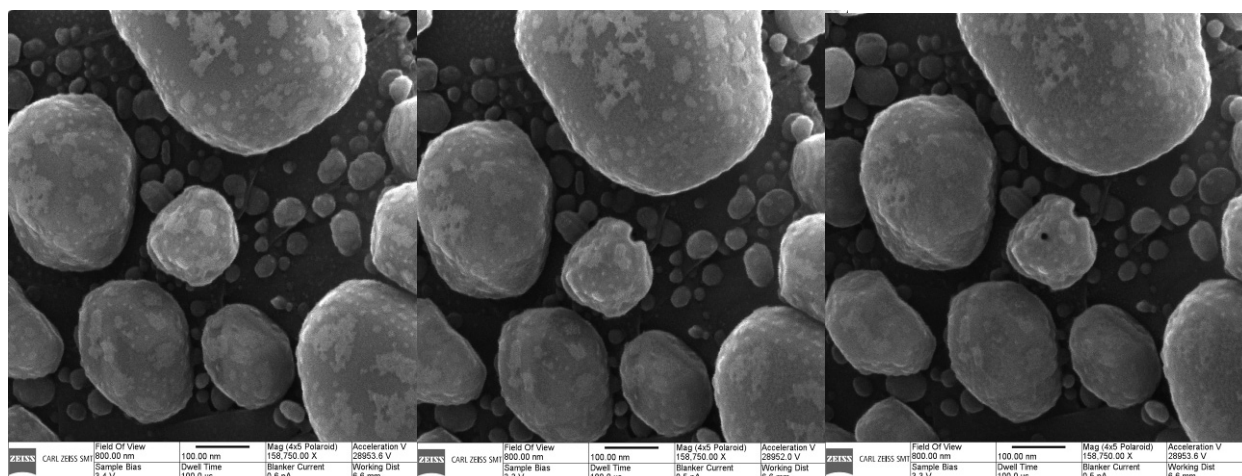


FIGURE 7. HIM SE images of He ion beam modification of nanostructures of a Pt-decorated gold-on-carbon sample. First image with no modification (left). After nano-milling at 2 o'clock position (center) and after drilling a 12 nm diameter hole (right). 800 nm field-of-view images.

Figure 7 is a series of images depicting the high precision material removal from gold on carbon sample using the HIM. This illustrates the effects of irradiation of approximately 3 pA beam current for approximately 60 seconds at 28 keV landing energy. Figure 7 (left) is the initial image taken with conditions conducive to imaging, whereas in Figure 7 (middle) the instrument conditions were changed to a very small scanned region (very high magnification image setting) for material removal. The small square region at the 2 o'clock location has been removed through irradiation with the helium ion beam. In Figure 7 (right), a small 10 nm hole was precisely milled near the center of the gold island in point irradiation mode thus, showing how precisely the beam can be positioned and material removed.

Semiconductor Imaging and Metrology

The potential of achieving higher resolution and greater surface sensitivity has prompted a great deal of interest in the HIM for semiconductor metrology applications. The SEM is currently the tool of choice for semiconductor production and sample charging is often an issue. Many samples in the SEM are prone to charging and charge reduction is commonly achieved by lowering the accelerating voltage down into the 1 kV range to achieve a charge balance [26]. The immediate result has, historically been, a significant reduction in resolution due to beam broadening. Hence, edge definition is also broadened. Modeling has been able to de-convolute edge information from the images, but requires an accurate model to be used in conjunction with the instrumentation obtaining the data. Aberration corrected SEMs working at low accelerating voltage may, in the near future, improve

upon this situation and this avenue is currently being explored, as well.

Semiconductor metrology with the HIM is different (today) in that the HIM only operates at high accelerating voltages. Therefore, no direct comparisons of the HIM and the SEM at low landing energy is possible. Figure 8 shows a comparison of linescans of conductive patterned amorphous silicon lines (upper) and the complementary SEM and HIM images (lower). The images (and linescans) were both taken at high landing energies and thus provides highly distinct edge definition as shown in the figure. The edge sharpness would be expected to be much higher than that of the low accelerating voltage SEM. Additional work to understand the proper conditions for semiconductor metrology with the HIM is ongoing.

The HIM benefits from the difference in specimen interaction to provide higher surface detail. Modeling of the ion beam interaction [16] has shown that in the helium ion microscope, the characteristics of the measurement profile are similar to those obtained from the SEM. Earlier work on x-ray mask structures [27] in the SEM with transmission electron detection demonstrated for the first time a “notch” structure apparent in the modeled linescan. This notch is a consequence of the electron beam generating signal as it scans along the sidewall. More recent modeling has shown this to be a characteristic of the SEM signal generation and now the HIM. Similarly, the modeling may relate to the time that the ion beam resides on the sidewall of the structure under test. But, since the HIM is potentially higher in resolution this characteristic

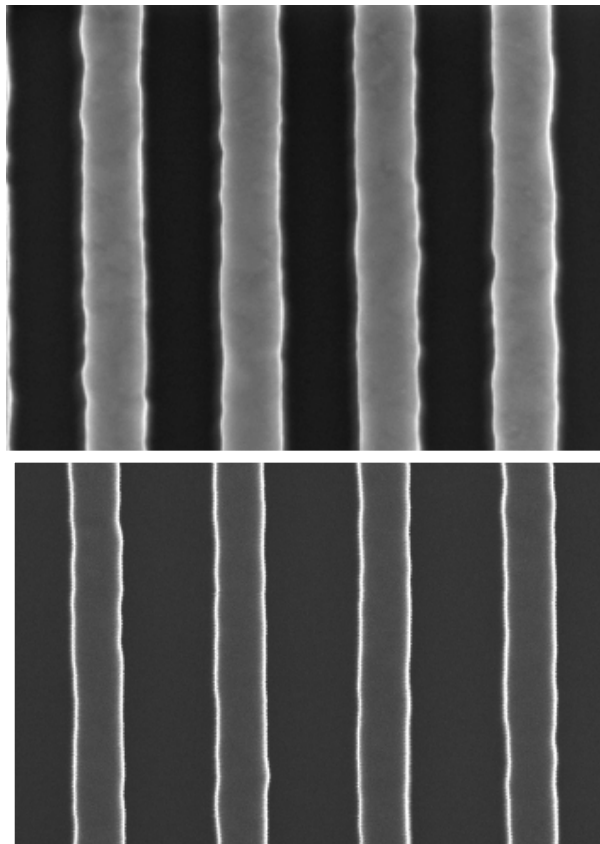
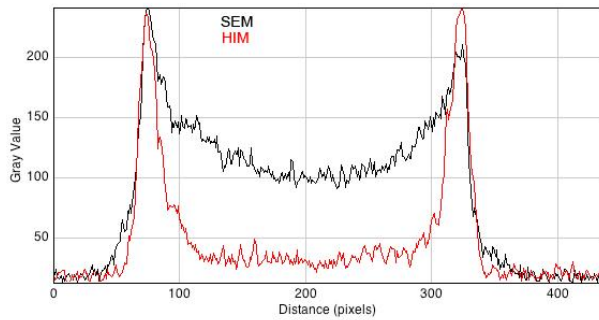


FIGURE 8. Comparison of the linescans of patterned amorphous silicon lines (top) and a complementary SEM (middle) and HIM (lower) images. The images (and linescans) were both taken at high landing energies. Note the more clearly (narrowly) defined edge in the HIM image (not the exact same set of lines). 1 μm field-of-view images.

may be more pronounced. The inflection point is thought to be a reproducible point and as such is being closely looked at as a possible fiducial to the location of the structure edge. This may potentially lead to an accurate measurement even without the benefit of modeling, but with some degree of measurement uncertainty still to be determined. Currently work in this area is also being pursued.

Charge Reduction

Current HIM instruments operate routinely at high accelerating voltages. Some semiconductor samples being viewed can build up a positive charge on the surface. Unlike the SEM, where the negative charge build-up can be quite high – high enough to detrimentally deflect the electron beam in some instances, the positive charging in the HIM can be eliminated or at least minimized by employing an electron flood gun. Operating conditions can be established to facilitate viewing materials such as photoresist with the flood gun. Figure 9 presents the results of HIM imaging of patterned photoresist structures on a silicon substrate. On the left is a tilted view of wide resist lines on Si. On the right is the image of 40 nm wide resist patterns showing considerable wall roughness. Typically, this type of sample would require use of a low voltage SEM due to the possibility of negative charge build-up, but with the HIM, these samples can be imaged without the disturbing sample charging by employing the electron flood gun.

The electron flood gun is also useful in imaging and metrology of chromium on quartz photomasks. Photomasks can be very difficult to image in the SEM due to charge build-up in the quartz. Postek et al. (2003) successfully used variable pressure SEM to dissipate the charge build-up for the imaging and metrology of chromium photomasks [28]. However, as shown in Figure 10, the HIM can also be successfully employed in the imaging and metrology of these samples. The positive charge build-up is removed by employing an electron flood gun, thus enabling high resolution imaging of the chromium photomasks (Figure 10). Optimization of the electron flood gun is currently being undertaken to determine the proper conditions for common semiconductor materials and the effects of this tool upon measurements made while it is being operated.

Helium Ion Beam Lithography

Pushing lithography to the limits is important to semiconductor manufacturing. Electron beam lithography (EBL) has been used in lithographic patterning for many years. EBL suffers from many of the same issues as secondary electron imaging such as exposure from backscattered electrons, SE2s and other fast secondary electrons. Focused ion beam lithography with a gallium source has not been used extensively for resist patterning mainly because of the resolution constraints. Helium ion lithography with ~ 200 nm resolution was demonstrated over 20 years ago, but it suffered from a lack of ion column

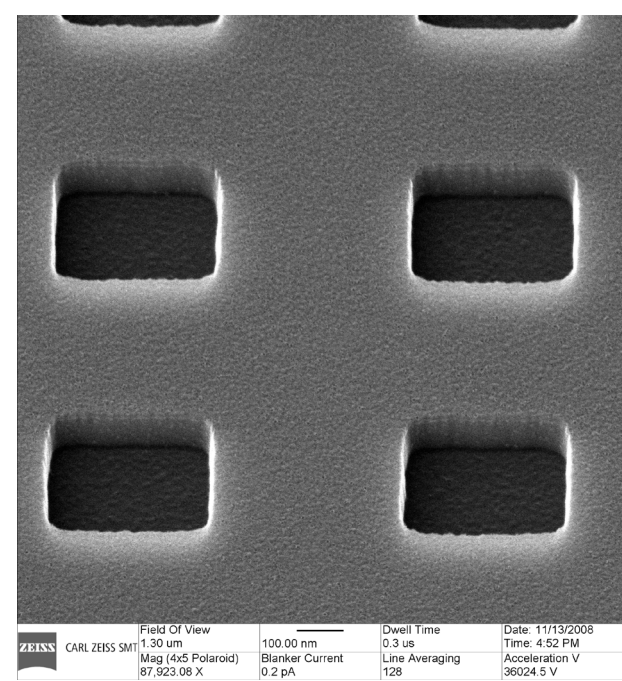
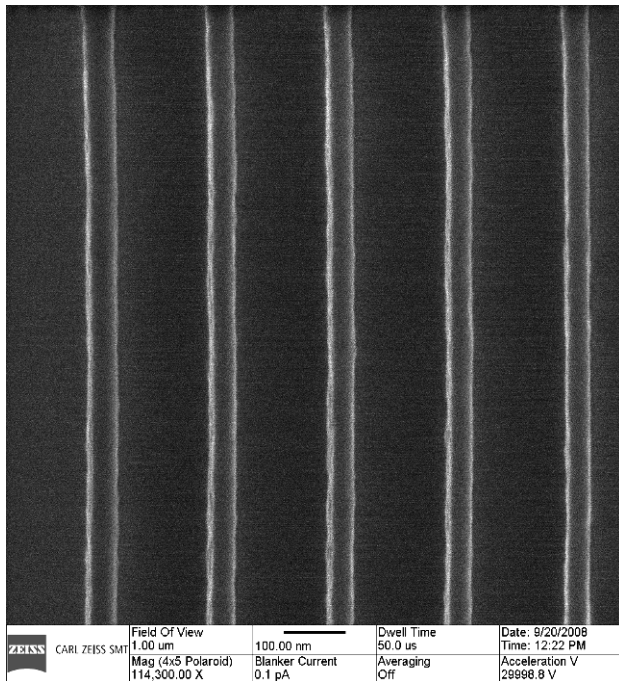
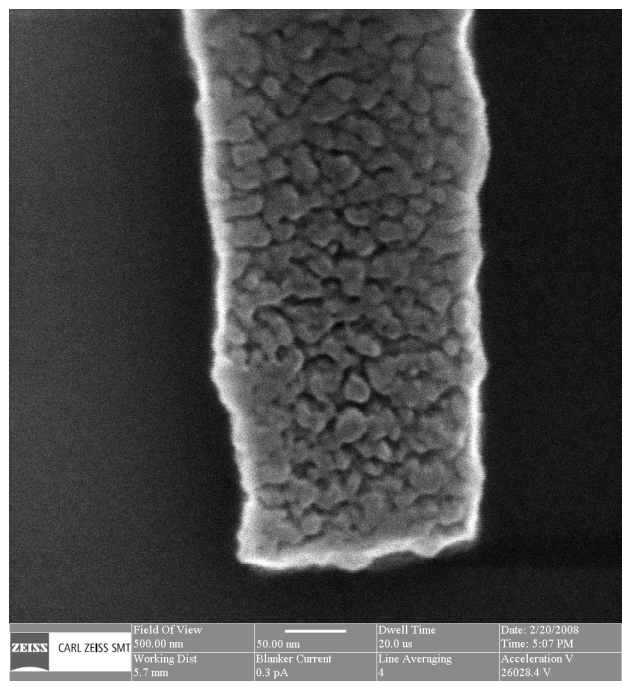
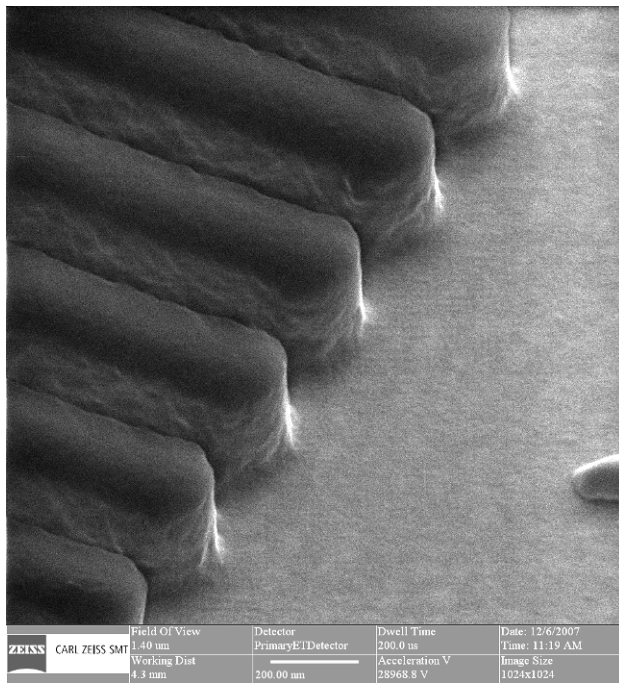


FIGURE 9. Tilted view of wide photoresist resist lines on Si with the use of the electron flood gun to reduce charging, 1.4 µm field of view (top); 40 nm wide resist patterns showing wall roughness, 0.1 pA beam current, 1 µm field-of-view (bottom). Please note that without the use of the flood gun significant charging would inhibit successful imaging.

FIGURE 10. HIM micrograph of a chromium on quartz photomask (top) 500 nm field-of-view and EUV mask (bottom) 1.3 µm field-of-view.

technology to make it a viable competition to EBL [29]. One advantage to using helium ions for lithography is the potential for higher resolution lithography than electrons [30]. The helium ion

microscope has demonstrated that it is capable of generating extremely fine lines with extremely straight walls due to the deep penetration of the helium ions into the substrate and the lack of additional secondary

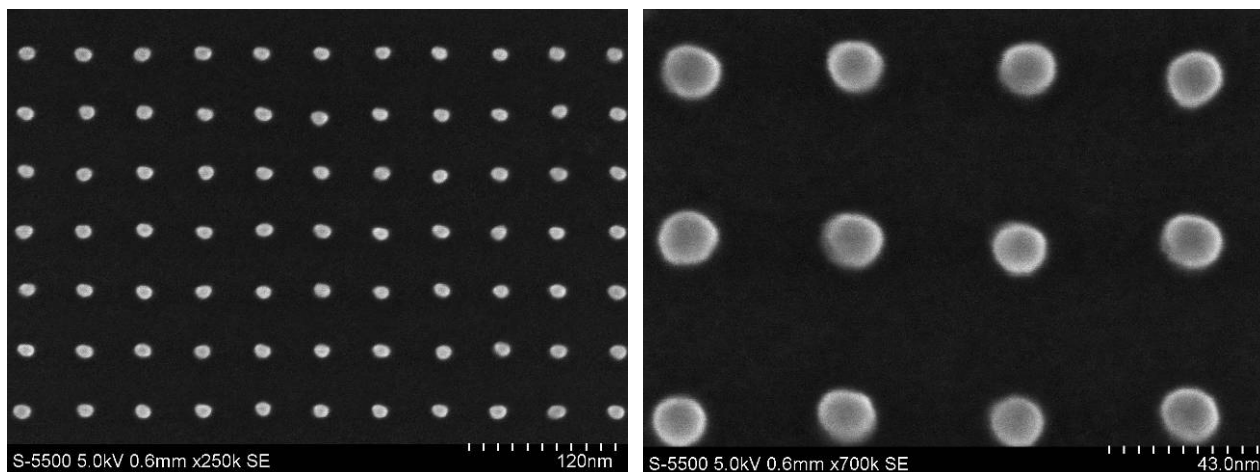


FIGURE 11. Helium ion beam lithography. Dense array of 15 nm hydrogen silsesquioxane (HSQ) resist posts generated by helium ion lithography 500 nm field of view (left) and 180 nm field-of-view (right).

signals which can degrade the lithographic fidelity. Figure 11 shows dense array of approximately 15 nm diameter hydrogen silsesquioxane (HSQ) resist posts generated by helium ion lithography. HSQ is a high resolution electron beam resist and it permits high-resolution SEM inspection following patterning and development. The helium ion beam lithography technology is in its beginnings but it has already demonstrated an ability to fabricate 10 nm lines with a 20 nm pitch [31]. There is still much to be done, but ion beam lithography shows promise and the sensitivity of the resist materials can be substantially higher, so higher –throughput direct lithography may be possible.

SUMMARY

In the interim between the original 2007, paper when the first commercial helium ion microscope was delivered to NIST was presented [7], a substantial evolution of the instrumentation has occurred. The performance of the instrument has markedly improved, as well as, the attainable resolution. Typically, the benchmark of performance for scanned beam instruments is the measure of resolution. But, it must be understood that where scanned particle beam instrumentation is concerned, resolution determination is more complicated than just laying a ruler on a micrograph and measuring the distance between two points. This concept is more involved than either the classical light microscope or even TEM. In this instance, the specimen plays a major part in the overall performance measure. Clearly, instrument performance is a strong issue and vast improvements in instrument design have strongly contributed to advances over the years in both SEMs and now the evolution of the HIM. Improved lens designs and

illumination sources have been the main contributors to increased SEM instrument performance. But, instrument resolution relies not only on a high performing instrument design, and instrument operating conditions, but also on the material being viewed to demonstrate successfully the performance characteristics. Particle beam interactions and the nature and manner of the signal being collected are major contributors, as well. Hence, sample choice plays a significant role to demonstrate the performance of any instrument. It is also likely that the perceived instrument resolution for each sample will vary depending upon the materials composing that particular sample. For that reason, specialized samples have been developed for the demonstration of resolution capabilities. These samples have had to evolve as did the instruments. But, one must always keep in mind that one sample may work better than another for a particular set of operating conditions or instrument design so one must be continually vigilant that fair evaluations are made.

Research to enable accurate measurements in the HIM is ongoing. Modeling of the HIM signal, just like the SEM signal, is crucial to the measurement capability and much progress has been made in that area. Precise measurements in either the SEM or the HIM can be accomplished as long as one is careful. As time progresses and more is understood about the imaging mechanisms in the HIM through experimentation and modeling, the advantages or disadvantages of this new instrument will become more apparent.

ACKNOWLEDGEMENTS

The authors would like to thank and acknowledge the collaboration with D. Winston and K. Berggren of

MIT, Cambridge, MA. on the HBL work and the strong collaborations afforded by Zeiss SMT, regarding the development of this paper and their commitment and continued efforts to improve instrumentation for nanotechnology and nanometrology. The authors would also like to thank both the NIST Office of Microelectronics Programs and International SEMATECH for partially funding this work.

REFERENCES

- Contribution of the National Institute of Standards and Technology; not subject to copyright.
- Certain commercial equipment is identified in this report to adequately describe the experimental procedure. Such identification does not imply recommendation or endorsement by the National Institute of Standards and Technology, nor does it imply that the equipment identified is necessarily the best available for the purpose.
- Interagency Working Group on manufacturing R&D workshop report: Instrumentation, Metrology and Standards for Nanomanufacturing. [Available for download at: www.manufacturing.gov], (2008)
- National Nanotechnology Initiative. NNI Grand Challenge Workshop Report. Instrumentation and Metrology. [Available for download at: www.nano.gov] (2006).
- M. T. Postek and K. Lyons. 2007, Proc. SPIE 6648, 664802-1 - 664802-7 (2007).
- D. C. Joy, B. Griffin, J. Notte, L. Stern, S. McVey, B. Ward and C. Fenner. Proc. SPIE 6518, 65181L-1 – 65181L-8 (2007).
- M. T. Postek, A. E. Vladar, J. Kramar, L. Stern, J. Notte, and S. McVey. *Frontiers of Characterization and Metrology for Nanoelectronics*, AIP Press CP931 American Institute of Physics (Seiler et al., eds) 161-167 (2007).
- M. T. Postek and A. E. Vladar, *SCANNING* 30:457-462. (2008).
- M. T. Postek, A. E. Vladar, J. Kramar, L. Stern, J. Notte and S. McVey Proc. SPIE. 6648, pp 664806-1 – 664806-6 (2007).
- Recently, the development of a new standard for the evaluation of image sharpness has begun through the International Organization for Standardization (ISO). Currently, a working committee of ISO is reviewing a draft documentary standard of software programs for the evaluation of image resolution in the SEM and HIM.
- A.E. Vladar, M. T. Postek and B. Ming. *Microscopy Today* 3:6-13.(2009)
- M. T. Postek, *The Scanning Electron Microscope. Handbook of Charged Particle Optics.* (ed. Jon Orloff) CRC Press, Inc., New York. 363-399.(1997).
- Published specifications for the Hitachi S-5500 SEM (<http://www.hitachi-hita.com/pageloader~type~product~id~389~orgid~42.html>).
- Helium Ion Microscopy. *Microscopy and Analysis* January 2009 p28 www.smt.zeiss.com/orion
- B. Ward, J. Notte, and N. Economou., *J. Vac. Sci. Technol. B* 24(6): 2871-2875.(2006).
- T. Yamanaka, K. Inai, K. Ohya and T. Ishitani, 2009. *Proc. SPIE* (2009) (in press).
- R. Ramachandra, B. Griffen, and D. C. Joy. Modeling for metrology with a helium beam. *Proc. SPIE* 6922: DOI: 1017/12.772300. (2008)
- R. Ramachandra, B. Griffen, and D. C. Joy *Ultramicroscopy* (in press).
- T. E. Everhart and M. S. Chung. *J. Appl. Phys.*, 43 (9):3707-3711. (1972).
- T. E. Everhart and P. H. Hoff.. *J. Appl. Phys.* 42(13): 5837-5846.(1971).
- F. Hasselbach, U. Rieke and M. Straub. 1983. *Scanning Electron Microscopy*, SEM Inc./1983/II. pp. 467-478 (1983).
- K.-R.Peters *Scanning Electron Microsc.* 1519-1544 (1985).
- D. Cohen-Tanugi and N. Yao, *J. Appl Phys* 104:063504-1 - 063504-7 (2008)
- H. Seiler, *J.Appl.Phys.*,54, R1-18 (1984)
- R. Baragiola, E. Alonso, A. Oliva-Florio *Phys.Rev B* 19, 121-129 (1979)
- M. T. Postek, SEM/1984/III, SEM, Inc. 1065 1074 (1984).
- M. T. Postek, J. R. Lowney, A. E. Vladár, W. J. Keery, E. Marx and R. D. Larrabee *NIST J. Res.* 98:415-445.(1993).
- M. T. Postek, and A. E. Vladar, A. E. Application of high pressure/environmental SEM microscopy for photomask dimensional metrology. *CP 683 Characterization and Metrology for ULSI Technology: 2003 International Conference* (D. Seiler et. al.eds) AIP Press, New York. (2003).
- D. Cohen-Tanugi and N. Yao, *J. Appl Phys* 104:063504-1 - 063504-7 (2008)
- K. Horiuchi, T. Itakura and H. Ishikawa, *J. Vac. Sci. & Tech. B*, 6, 241-244 (1988).
- D. Winston, B. Cord, M. Mondol, J. Yang, K. Berggren, B. Ming, A. Vladar, M. Postek, D. Bell, W. DiNatale and L. Stern. *J. Vac. Sci. & Tech.*(in press).